Supplementary Information (SI)

Structure of the neutral red crystal with water molecules

Very thin red ribbon like neutral red crystals were grown only in the presence of microorganisms. Our attempts to grow single neutral red crystals from aqueous and non-aqueous solvents did not yield any crystalline products. Most trials resulted in amorphous precipitation. The weak data from these thin crystals, however, revealed the non-hydrogen atom positions unambiguously showing a neutral red molecule and four water molecules. The unique arrangement of a double row of water molecules on either side of the crystal molecule with their N(phenazine)…O(water) and O(water)…O(Water) short contacts indicated an intricate H-bonding network (Fig. S6 a).

The 'ladders' formed by water molecules O1W … O2W and O3W…O4W along the screw (b-) axis hook the neutral red molecules at central ring nitrogen atoms N2 and N3 at their nodes. The positions of the H-atoms, particularly in this weak X-ray data, were not possible to locate from the difference Fourier map. Therefore, H-atoms on the four water molecules were modelled, so as to satisfy all the possible donor-acceptor interactions in this arrangement. Both the ladders, similar in their framework, are shown in Fig. S6 (b and c) and the geometrical parameters of the H-bonding are given in Table S1.

In modelling the H-atoms, the most probable position is of the H-atom that would make O-H…N contacts, O4w-H4Wa…N2 (similarly, O1W-H!Wa… N3). The rest of the water H-atoms can build the same ladder with different roles played by the donor acceptors in making O-H…O contacts. This implies a possible dynamic situation of protons in the water network, where the protons can exchange their roles in real time without change in the Oxygen positions. The two infinite one dimensional ladders hold pi…pi stacked neutral red molecules by O-H…N contact at each of their 'nodes' (Fig. S6 d-f). The pi…pi interaction between two successive molecules is due to the overlap of two rings, the central and one of the side rings

(Fig. S6 e) with the centroid to centroid distance being 3.593 A (centroids are calculated for the entire two ring fragment involved in the interaction). The stacked neutral red molecules make ~ 45 with the ladder axis (b-axis).

The packing of the neutral red molecules along with the water ladders in the crystal lattice is remarkable, which appears to be a nano wired assembly conducive for transfer of protons through the water channels to the nitrogens of the neutral red molecule. The crystallization of the entire assembly of the achiral dye molecule in a chiral space group P2(1) rather than a centrosymmetric one is also striking in this context. The neutral red molecules that are held at the central N atoms by O-H N contacts also make additional short contacts from both the ends (Fig. S6 g) that would help to keep the orientation of the molecules fixed in the structure. The geometry of these interactions is given in Table 1S. The packing of molecules viewed down the b-axis shows the remarkable organization of water and neutral red molecules in the crystal lattice strongly suggesting this to be a more functional assembly for proton transfer than merely a solvate structure.

Figure Legends

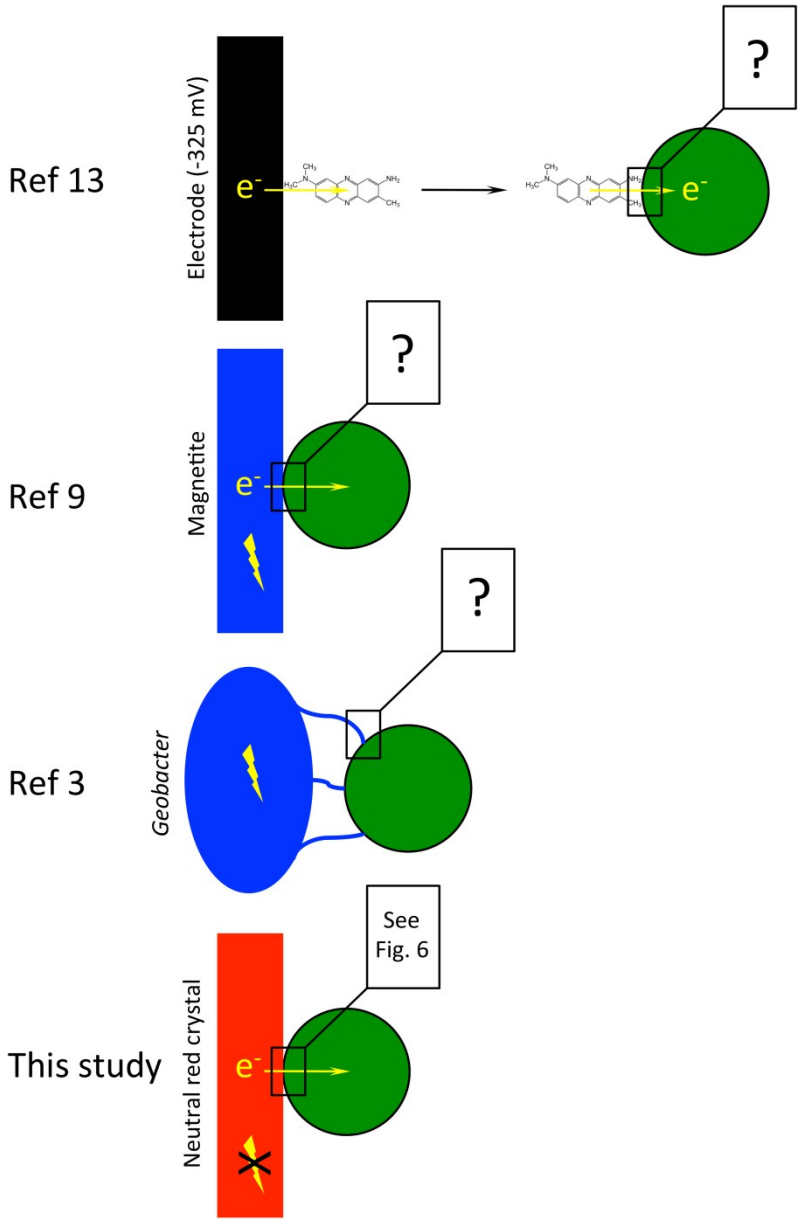

Figure S1 | Cartoon illustration of conceptual differences between 1) soluble electron shuttle mediated enhancement of methanogenesis[13], 2) conductive material mediated enhancement of methanogenesis[9], 3) DIET mediated enhancement of methanogensis[3] and 4) neutral red crystal mediated enhancement of methanogenesis (this study).

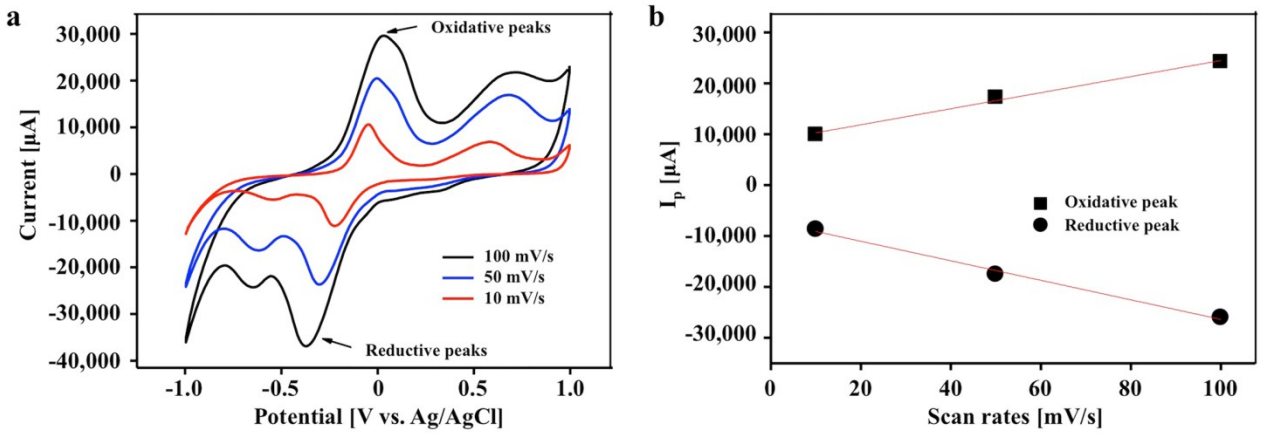

Figure S2 | Cyclic voltammogram and dependency of scan rate of Neutral Red Crystals. a, Cyclic voltammogram of crystalline neutral red in association with the working electrode in an electrochemical cell with different scan rates. b, Scan-rate dependence of the oxidative (closed squares) and reductive (closed circles) peak currents (I_p) of crystalline neutral red from the CV.

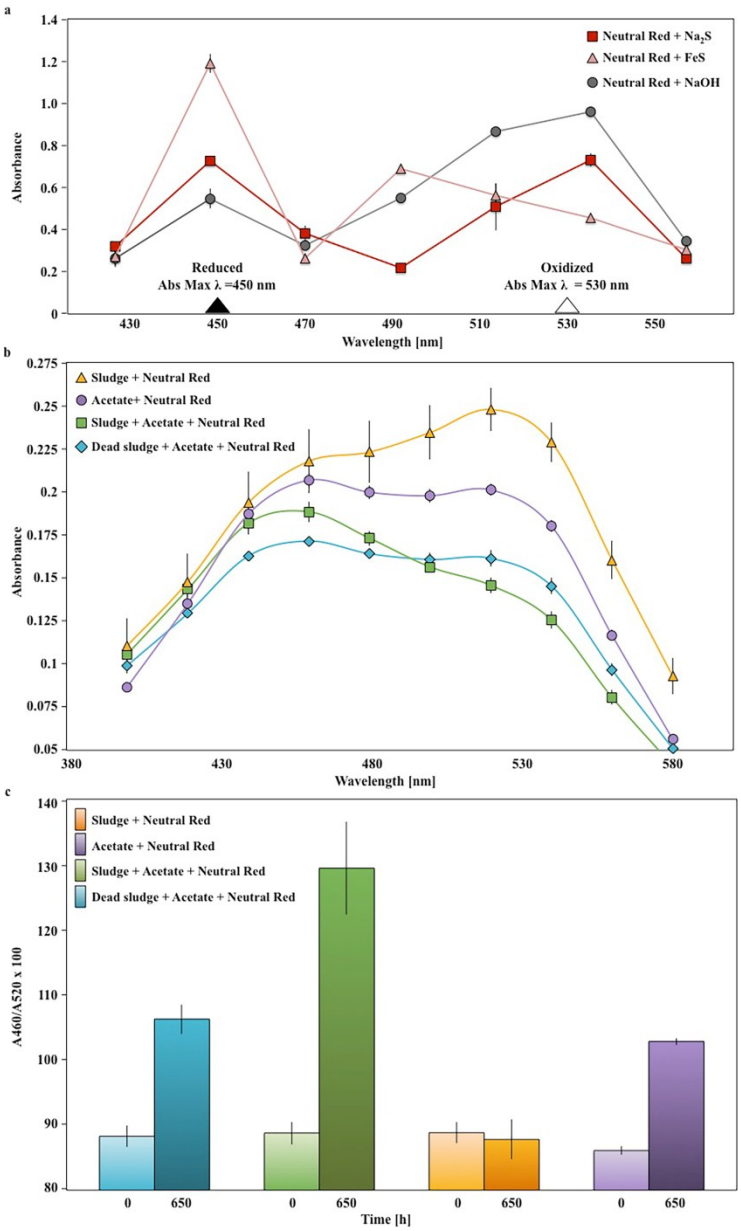

Figure S3 | Reduction processes of neutral red. a, Reduction of neutral red (250 µM) by soluble sulfide and iron sulfide. The reduced form of neutral red was observed at 450 nm using soluble sulfide (Na_2S, red squares) or iron sulfide (FeS, pink triangles) for the reduction process at pH 7. b-c, Reduction of neutral red by acetate fed activated sludge (green squares and bares), acetate treated dead sludge (blue diamonds and bars) and acetate amendment (purple circles and bars). Oxidation of neutral red by not treated sludge (yellow triangles and bars). Error bars represent standard deviation (n = 3).

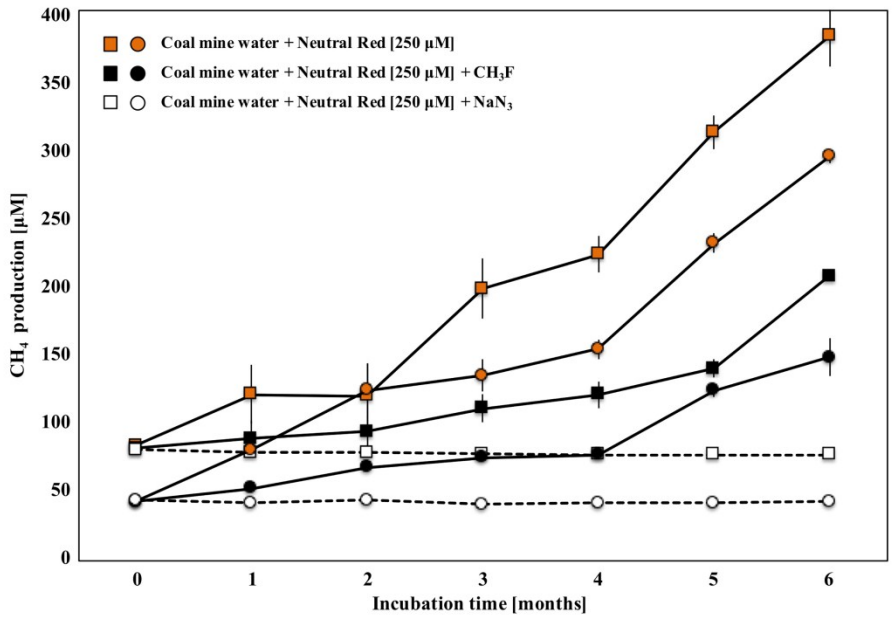

Figure S4 | Inhibition of neutral red enhanced methane production in coal fed groundwater cultures. Acetoclastic methane production was inhibited using methyl fluoride (CH_3F, black square and circle) in two different neutral red enhanced coal fed groundwater cultures (orange square and circle).

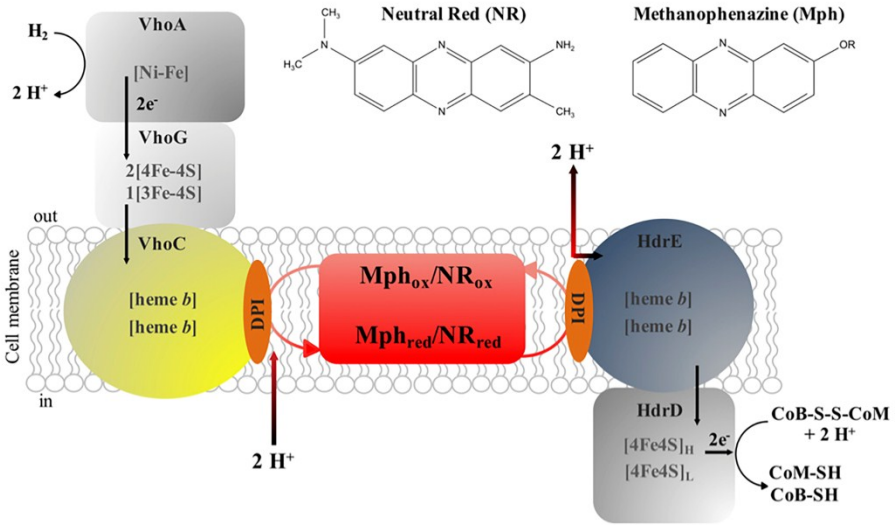

Figure S5 | Neutral Red–Methanohenazine substitution mechanism in *Methanosarcinales*. Model for mechanism by which NR is involved into the respiratory chain of *Methanosarcina mazei* and substitutes *Methanophenazine* (Mph). Oxidized Neutral Red (NR_{ox}) is reduced by Vho hydrogenase (Vho) to reduced Neutral Red (NR_{red}) in a process that involves extracellular hydrogen oxidation and electron transfer to NR_{ox}. NR_{red} interacts with the heterodisulfide reductase complex (Hdr) and serves as electron donor for the reduction of CoM-S-S-CoB and thus the regeneration of the methanogenic cofactors CoM-SH and CoB-SH.

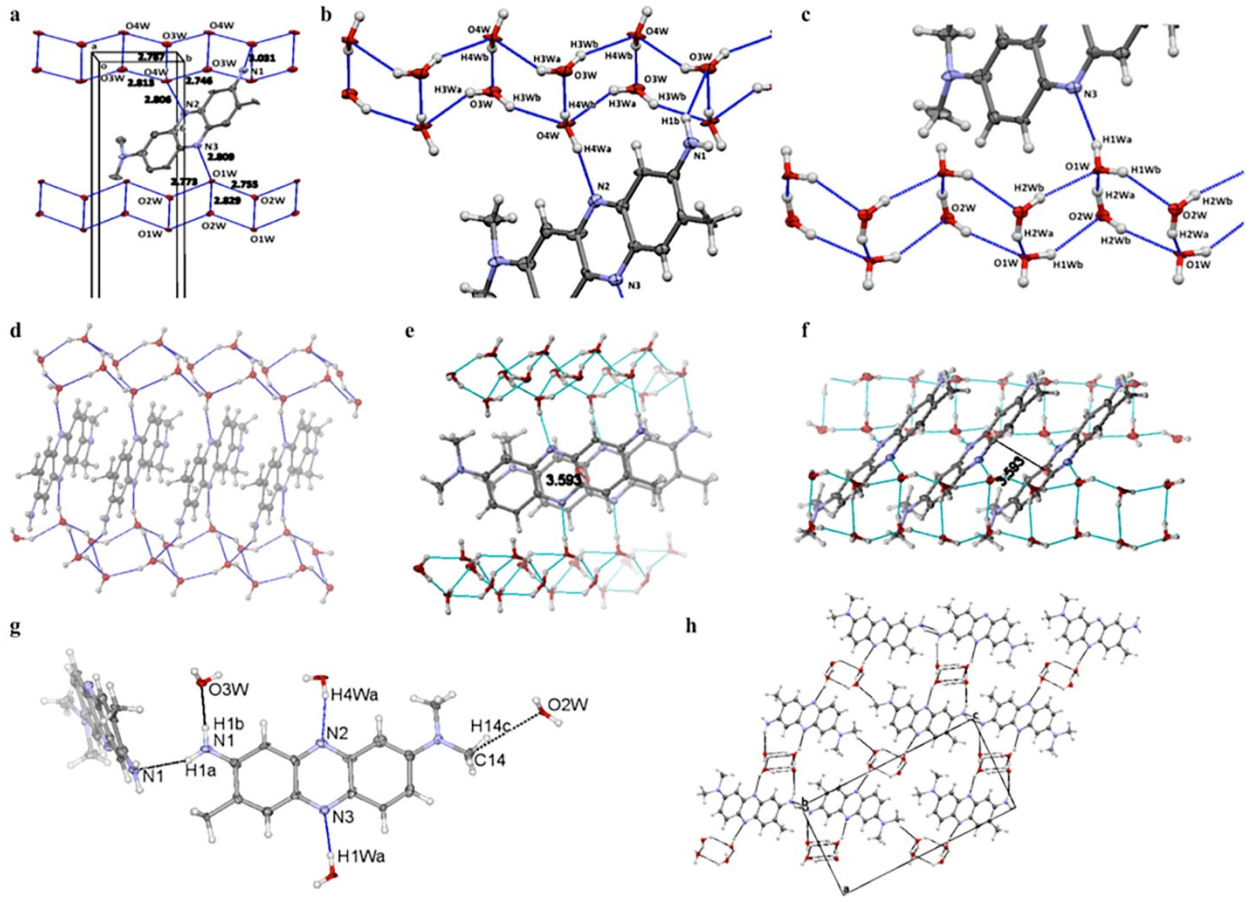

Figure S6 | Structure of the Neutral Red Crystal with water molecules. a, The unique arrangement of a double row of water molecules on either side of the neutral red molecule with their N(dye)…O(water) and O(water)…O(Water) short contacts indicated an intricate H-bonding network. Zoom in view of upper and lower half of water ladders b, with waters O3W…O4W and c, O1W…O2W. d-f, Water ladders holding the red dye molecules by O-H…N bonds. Packing of molecules viewed down two-fold screw axis with g, significant short contacts of a single molecule and h, packing of molecules in the unit cell viewed down b-axis.

Tables

Table S1 | H-bond geometry (Å, º). Symmetry codes: (i) −*x*, *y*+1/2, −*z*; (ii) −*x*+1, *y*+3/2, −*z*; (iii) *x*+1, *y*−1, *z*; (iv) *x*, *y*+1, *z*; (v) −*x*, *y*−1/2, −*z*+1; (vi) −*x*+1, *y*+1/2, −*z*; (vii) *x*, *y*−1,*z*.

D—H···*A*	*D*—H	H···*A*	*D*···*A*	*D*—H···*A*
N1—H1*a*···N1^{i}	0.88	2.35	3.171 (8)	156 (1)
N1—H1*a*···C3^{i}	0.88	2.78 (1)	3.480 (10)	137 (1)
N1—H1*b*···O3*W*^{ii}	0.88	2.27 (1)	3.032 (7)	144 (1)
C14—H14*c*···O2*W*^{iii}	0.98	2.55 (1)	3.485 (10)	160 (2)
O1*W*—H1*Wa*···N3	0.85	2.00 (2)	2.809 (7)	159 (5)
O1*W*—H1*Wb*···O2*W*^{iv}	0.85	2.02 (4)	2.755 (6)	144 (7)
O2*W*—H2*Wa*···O1*W*^{v}	0.85	2.19 (6)	2.829 (6)	132 (6)
O2*W*—H2*Wb*···O1*W*	0.85	2.00 (2)	2.772 (6)	151 (4)
O4*W*—H4*Wa*···N2	0.85	2.01 (2)	2.807 (7)	155 (4)
O4*W*—H4*Wb*···O3*W*^{vi}	0.85	1.99 (2)	2.785 (7)	156 (4)
O3*W*—H3*Wa*···O4*W*^{vii}	0.85	1.99 (2)	2.746 (7)	147 (3)
O3*W*—H3*Wb*···O4*W*	0.85	2.02 (2)	2.813 (7)	156 (4)